

# Crystal Structure of Rat GTP Cyclohydrolase I Feedback Regulatory Protein, GFRP

Gerd Bader<sup>1</sup>, Susanne Schiffmann<sup>2</sup>, Anja Herrmann<sup>2</sup>, Markus Fischer<sup>2</sup>  
Markus Gütlich<sup>2</sup>, Günter Auerbach<sup>1</sup>, Tarmo Ploom<sup>1</sup>, Adelbert Bacher<sup>2\*</sup>  
Robert Huber<sup>1</sup> and Thorsten Lemm<sup>1</sup>

<sup>1</sup>Abteilung Strukturforschung  
Max-Planck-Institut für  
Biochemie, Am Klopferspitz  
18a, D-82152 Martinsried  
Germany

<sup>2</sup>Lehrstuhl für Organische  
Chemie und Biochemie  
Technische Universität  
München, Lichtenbergstr. 4  
D-85747 Garching, Germany

Tetrahydrobiopterin, the cofactor required for hydroxylation of aromatic amino acids regulates its own synthesis in mammals through feedback inhibition of GTP cyclohydrolase I. This mechanism is mediated by a regulatory subunit called GTP cyclohydrolase I feedback regulatory protein (GFRP). The 2.6 Å resolution crystal structure of rat GFRP shows that the protein forms a pentamer. This indicates a model for the interaction of mammalian GTP cyclohydrolase I with its regulator, GFRP. Kinetic investigations of human GTP cyclohydrolase I in complex with rat and human GFRP showed similar regulatory effects of both GFRP proteins.

© 2001 Academic Press

**Keywords:** GTP cyclohydrolase I; tetrahydrobiopterin; biosynthesis; regulation; X-ray structure

\*Corresponding author

## Introduction

GTP cyclohydrolase I (E.C. 3.5.4.16) catalyses the conversion of guanosine triphosphate (GTP) to dihydroneopterin triphosphate (H<sub>2</sub>NTP), the initial and rate limiting step in the *de novo* synthesis of tetrahydrobiopterin (BH<sub>4</sub>). BH<sub>4</sub> is an essential cofactor for phenylalanine hydroxylase, tyrosine hydroxylase and tryptophane hydroxylase<sup>1</sup> and can affect the rate of biosynthesis of neurotransmitters such as serotonin or dopamine and hormones like melatonin *via* its intracellular concentration. Furthermore, BH<sub>4</sub> serves as a cofactor in all three forms of nitric oxide synthase<sup>2</sup> and glycerol ether monooxygenase.<sup>3</sup> As BH<sub>4</sub>, unlike other cofactors, is one of the regulators of these enzymic reactions,<sup>4</sup> it plays an important role in the control of phenylalanine catabolism and of neural and immune

functions. Disorders in BH<sub>4</sub> synthesis are associated with serious neuronal diseases such as hyperphenylalaninemia.<sup>5</sup> The intracellular BH<sub>4</sub> concentration is controlled by the rate of its *de novo* synthesis<sup>1</sup> by GTP cyclohydrolase I through transcriptional<sup>6</sup> and substrate<sup>7</sup> level regulators.

Mammalian GTP cyclohydrolase I is subject to feedback inhibition by BH<sub>4</sub> mediated by complex formation with GTP cyclohydrolase I feedback regulatory protein (GFRP).<sup>8</sup> In the presence of GFRP and GTP, BH<sub>4</sub> inhibits GTP cyclohydrolase I while phenylalanine stimulates the enzyme.<sup>9</sup> This mode of GTP cyclohydrolase I regulation provides a mechanism to regulate phenylalanine catabolism and to avoid toxic accumulation of phenylalanine. BH<sub>4</sub> synthesis is also inhibited by various other pterins. The prototypic inhibitor 2,4-diamino-6-hydroxypyrimidine (DAHP) has been shown to act by a dual mechanism, dependent on, and independent of GFRP.<sup>4</sup> However, recent findings indicate, that the regulation of GTP cyclohydrolase I activity might be different in different cell types as no GFRP mRNA was detectable in dopaminergic neurons.<sup>10</sup> It has also been shown that mammalian GTP cyclohydrolase I gets phosphorylated *in vivo*,<sup>11</sup> and that phosphorylation modulates GTP cyclohydrolase I activity.<sup>12</sup> GFRP has been purified, sequenced and cloned from rat liver.<sup>9</sup> Crosslinking and sedimentation experiments indicate that the 9.5 kDa protein forms a pentamer.<sup>13</sup> Gel filtration and enzyme activity measurements indicate that in

Present addresses: G. Auerbach, Antisense Pharma GmbH, Josef-Engert-Str. 9, D-93053 Regensburg, Germany; A. Herrmann, Microcoat GmbH, Am Neuland 1, D-82347 Bernried, Germany; T. Lemm, Roche Diagnostics, D-82327 Tutzing, Germany.

Abbreviations used: BH<sub>4</sub>, tetrahydrobiopterin; H<sub>2</sub>NTP, dihydroneopterin triphosphate; GFRP, GTP cyclohydrolase I feedback regulatory protein; DAHP, 2,4-diamino-6-hydroxypyrimidine; CBP, calmodulin-binding peptide.

E-mail address of the corresponding author: adelbert.bacher@ch.tum.de

both the inhibitory and the stimulatory complex the number of GFRP molecules equals that of the GTP cyclohydrolase I monomers. Mammalian GTP cyclohydrolase I forms decameric complexes similar to that of *Escherichia coli*,<sup>14,15</sup> suggesting that the regulatory complex consists of a GTP cyclohydrolase I decamer sandwiched between two GFRP pentamers.<sup>16</sup>

### Overall structure

The structure of GFRP has been solved and refined to a crystallographic *R*-factor of 16.3% ( $R_{\text{free}} = 21.1\%$ ) in the resolution range of 20–2.6 Å by the multiple isomorphous replacement technique using three derivatives. (Table 1). The structure has also been solved in a second, cubic crystal form and was refined to an *R*-factor of 21.7% ( $R_{\text{free}} = 26.5\%$ ) showing no significant differences between the two crystal forms. GFRP forms a pentamer of identical subunits (Figure 1). Each subunit consists of all the residues of the rat sequence, with the N-terminal Met being cleaved off post-translationally. A monomer is folded into an  $\alpha/\beta$ -structure with a dominant six-stranded antiparallel  $\beta$ -sheet. Between the strands S2 and S3, a short helix (H1, residues 25–31) and between the strands S4 and S5 a longer helix (H2, residues 52–60) are inserted. Both helices are located on the same side of the  $\beta$ -sheet. The monomers form a propeller-like pentamer with helix H2 located in the interface between the subunits. The pentamer forms a bent disk with convex and concave surfaces. The approximate dimensions are

50 Å × 50 Å × 20 Å. Within the loop connecting S1 and S2, a bound metal ion coordinated to the backbone carbonyl groups of Gln9, Arg11, Val14 and the side-chain oxygen atom of Thr8 with distances of 2.8 Å (Gln9), 2.9 Å (Arg11), 2.9 Å (Val14) and 3.0 Å (Thr8) was found. Furthermore, the backbone carbonyl group of Gly15 and a water molecule are 3.5 Å away. The coordination can best be described as a distorted, incomplete pentagonal bipyramid. The nature of this ion could not be determined unambiguously, but as no metal apart from potassium could be identified by total reflection X-ray fluorescence, it was modelled as a potassium ion from the crystallisation buffer. Between the strands S3 and S4, the residues 37–44 form a long, yet well-defined loop protruding away from the pentamer.

Upon oligomerisation, 34.5% of the monomer surface is buried. The interface is composed of a mixture of hydrophobic and hydrophilic interactions. The innermost strand of the propeller-like structure, S5 contacts the equivalent strand of the neighbouring monomers and the helix H2 contacts the loop connecting S2 to H1 and His81 at the C terminus.

### Proposed complex formation with GTP cyclohydrolase I

The known GFRP sequences are highly homologous (Figure 2), suggesting that interactions between GTP cyclohydrolase I and its regulatory protein are similar in these species. Rat GFRP regulates human GTP cyclohydrolase I as well as a del-

**Table 1.** Data collection, phasing and refinement of the orthorhombic crystal form

	NAT1	Thiomersal	KAu(CN) <sub>2</sub>	K <sub>2</sub> Pt(NO <sub>2</sub> ) <sub>2</sub> (NH <sub>3</sub> ) <sub>2</sub>
<i>A. Data collection</i>				
Resolution (Å)	2.6	2.7	2.8	2.8
Completeness	97.7	93.2	93.1	99.8
Total reflections	154,398	99,236	82,213	106,804
Unique reflections	14,719	13,106	11,856	13,107
$R_{\text{sym}}$ (%) <sup>a</sup>	11.8	12.8	7.6	17.9
<i>B. Phasing statistics</i>				
$R_{\text{iso}}$ (%) <sup>b</sup>	-	21.7	17.9	18.1
$R_{\text{C}}$ (%) <sup>c</sup>	-	0.74	0.80	0.87
Phasing power	-	1.38	1.16	0.50
No. of sites	-	5	2	1
<i>C. Refinement statistics</i>				
No. of protein atoms		3340		
No of solvent molecules		255		
No. of metal atoms		5		
No. of reflections		14070		
r.m.s.d bond length (Å)		0.007		
r.m.s.d bond angles (deg.)		1.38		
r.m.s.d. between monomers $C^{\alpha}$ (Å)		0.32		
Average <i>B</i> value (Å <sup>2</sup> )		22.03		
<i>R</i> -factor		16.1		
$R_{\text{free}}$ <sup>d</sup>		21.4		
<sup>a</sup> $R_{\text{sym}} = \frac{\sum_{hkl} \sum_i  I(hkl)_i - \langle I(hkl) \rangle }{\sum_{hkl} \sum_i I(hkl)_i}$ . <sup>b</sup> $R_{\text{iso}} = \frac{\sum_{hkl}  F_{\text{PH}}(hkl) - F_{\text{P}}(hkl) }{\sum_{hkl} F_{\text{P}}(hkl)}$ . <sup>c</sup> $R_{\text{C}} = \frac{\sum_{hkl}   F_{\text{PH}}(hkl)  + -  F_{\text{P}}(hkl)   - F_{\text{Hcalc}}(hkl) / \sum_{hkl}   F_{\text{PH}}(hkl)  + -  F_{\text{P}}(hkl)  }$ . <sup>d</sup> For 5% of the reflections.				

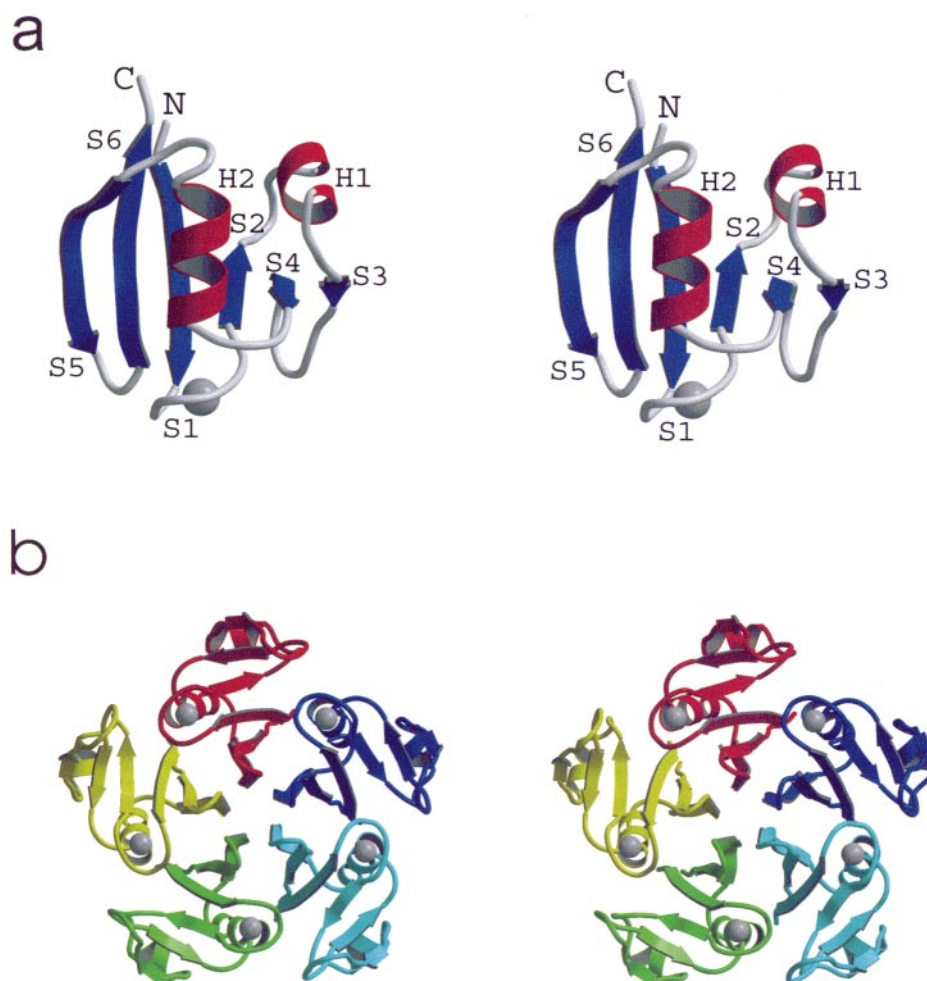


**Figure 1.** Structure of rat GFRP. (a) Stereoview of the GFRP monomer. (b) Stereoview of the GFRP pentamer from the bottom side. The bound metal ion is depicted in grey.

etion mutant of GTP cyclohydrolase I shortened N-terminally by 41 residues at the same level. Comparison of the surface potentials of rat GFRP and the recently solved N-terminally shortened mutant of human GTP cyclohydrolase I allow us to speculate about the mode of interaction between the GFRP pentamer and human GTP cyclohydrolase I (Figure 3). The contact surface of human GTP cyclohydrolase I is mainly positively charged (red colour). The convex surface of GFRP (Figure 3(a)) is also positively charged while the concave bottom of the pentamer displays a neutral to negative surface potential (Figure 3(c), blue colour). Therefore the interaction of GFRP with human GTP cyclohydrolase I is likely *via* its concave side. Docking of GFRP to the GTP cyclohydrolase I structure containing the residues 57-250 of the original human GTP cyclohydrolase I sequence with FTDOCK<sup>17</sup> yielded a model complex with the expected binding mode (Figure 4). Electrostatic interactions were considered as implemented in FTDOCK, i. e. of the backbone atoms terminal nitrogen and oxygen atoms are assigned a charge of 1 and  $-1$ , and peptide nitrogen

and oxygen atoms get a charge of 0.5 and  $-0.5$ , respectively. Furthermore, charges are assigned to the side-chain atoms Arg-N<sup>n</sup> (+0.5), Glu-O<sup>e</sup> ( $-0.5$ ), Asp-O<sup>d</sup> ( $-0.5$ ), Lys-N<sup>s</sup> (+1.0) and Pro-N ( $-0.1$ ). The above mentioned docking solution was the only biochemically reasonable solution, i. e. with the GFRP-pentamer located on the 5-fold symmetry axis of the cyclohydrolase decamer. Applying varying parameters in FTDOCK no other reasonable complex, most notably no complex with the convex side of GFRP bound to GTP cyclohydrolase I, was found.

In the aforementioned model, the exposed loop between the strands S3 and S4 binds into the cleft formed by two neighbouring cyclohydrolase monomers. All the three non-conservative substitutions of rat GFRP compared to the human sequence do not participate in the proposed binding site, thus supporting an identical regulatory mechanism in rat and man. The bound metal ion is part of the proposed interface, but the functional role, if any, of the metal ion is unclear. Kinetic studies failed to show a dependence of the functional properties on any metal ion. The mutation of Thr8,

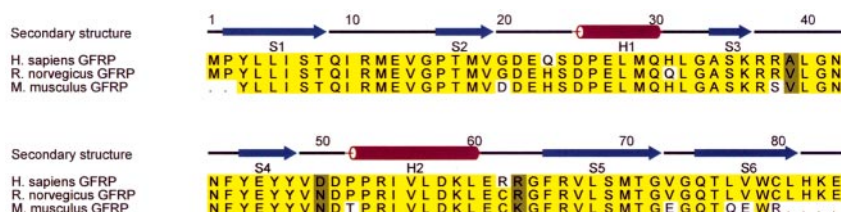


**Figure 2.** Sequence comparison of putative GTP cyclohydrolase I regulatory proteins. Conservative substitutions are shaded grey.

the only residue coordinating the metal ion *via* its side-chain, to alanine led to a complete loss of protein expression. This might indicate a role of metal binding in structure stabilisation or protein folding. Regarding the coarseness of such a rigid body docking experiment, we feel that a more detailed discussion of the docked complex in respect of single amino acid side-chain conformations is not appropriate, as it would be a significant over-interpretation of the available data. On the basis of the complex model, we cannot speculate on a possible binding side for phenylalanine.

### Regulatory properties of GFRP

To account for possible biochemical differences between the rat and human protein, the rat sequence was mutated to the human sequence. To verify our model of GFRP binding to human GTP cyclohydrolase I, calmodulin-binding peptide (CBP), a 21 amino acid residue C-terminal fragment from muscle myosin light-chain kinase was fused to the N terminus of human GFRP with a linker of 15 amino acid residues. During the purification process 19 amino acid residues were cleaved off at the N terminus, leaving a 17 amino acid residue CBP-fragment attached to GFRP. As the N termini of the monomers protrude from the top side of the GFRP pentamer, the CBP-linker-fragment should prevent binding to human GTP cyclohydrolase I with this side. Gel filtration experiments with the CBP-GFRP fusion protein and human GTP cyclohydrolase I revealed that the GFRP-GTP cyclohydrolase I complex is still formed, supporting the proposed side of complex formation.

Kinetic investigations of human GTP cyclohydrolase I in complex with rat GFRP or human

CBP-GFRP showed that both proteins regulate human GTP cyclohydrolase I of the same order of magnitude. Upon addition of  $\text{BH}_4$  to a mixture of the respective proteins with GTP, the specific activity of human GTP cyclohydrolase I drops from  $135 \text{ nmol min}^{-1} \text{ mg}^{-1}$  to  $3 \text{ nmol min}^{-1} \text{ mg}^{-1}$  in the case of rat GFRP and from  $85 \text{ nmol min}^{-1} \text{ mg}^{-1}$  to  $7 \text{ nmol min}^{-1} \text{ mg}^{-1}$  in the case of the human CBP-GFRP fusion protein. To strengthen our arguments further, hisactophilin, a 119 amino acid residue protein from *Dictyostelium discoideum* was fused to the N terminus of human GFRP. The resulting fusion protein showed regulatory effects of the same order of magnitude as the CBP-GFRP fusion protein.

As the GTP-binding sites of human GTP cyclohydrolase I lie approximately  $30 \text{ \AA}$  away from the potential GFRP-binding site (Figure 4) and the phenylalanine-binding sites are still unknown, the precise regulatory mechanism requires further investigation.

### Structural homologues

A search for related structures with the program DALI<sup>18</sup> did not reveal biologically significant structural homologies. Only three structures with a Z-score  $\geq 3$  were reported; the closest homologue with a Z-score of 3.8 is *E. coli* YciH (PDB entry 1D1R), a putative translation initiation factor.

### Materials and Methods

#### Protein expression and purification

The cDNA for the rat GFRP was cloned by reverse transcriptase polymerase chain reaction yielding a PCR product of 255 bp encompassing the open reading

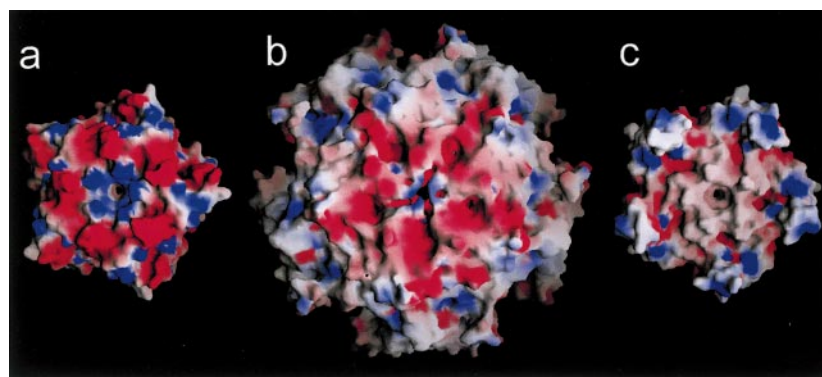


**Figure 3.** Electrostatic potentials. (a) Top side of rat GFRP. (b) Human GTP cyclohydrolase. I. (c) Bottom side of rat GFRP. Positive charges are shown in red, negative charges in blue.

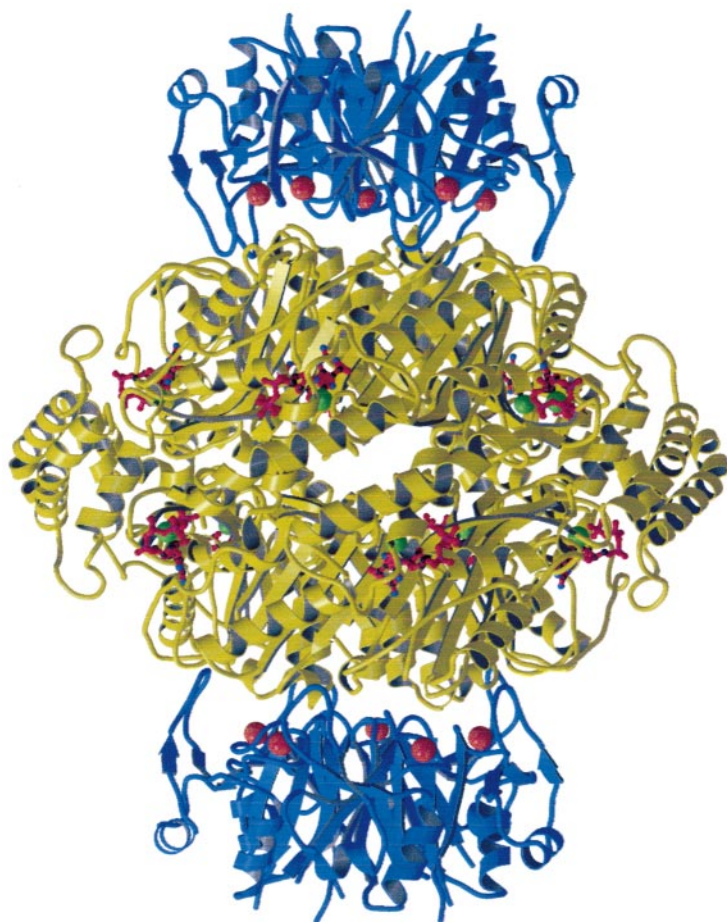


**Figure 4.** Model of the complex of GFRP (blue) and human GTP Cyclohydrolase I (yellow). The potassium ions in the interface region are depicted in red. The position of the bound GTP (red) is deduced from the homologous *E. coli* structure.

frame. The amplificate was ligated into pQE7 (Quiagen) and expressed in *E. coli* XL1. The recombinant GFRP was purified in a three-step procedure by heat precipitation (72 °C) followed by anion exchange chromatography (Q-Sepharose), the column was washed with buffer A containing 50 mM Tris-HCl and 2 mM dithioerythritol (DTE) and developed with a linear gradient of 0 to 500 mM KCl in buffer A. As final purification step the protein was applied to a gel filtration column (Superdex 75 C, Pharmacia) and eluted with 100 mM potassium phosphate, 2 mM DTE (pH 7.4). The rat sequence was mutated to the human sequence by PCR and purified as described. Calmodulin-binding peptide and hisactophilin were fused to the N-terminus of the human sequence in pNCO and expressed in *E. coli* XL1-Blue cells. The CBP-GFRP fusion protein was purified by cation exchange chromatography (Sephacrose SP Fast Flow) with 50 mM potassium phosphate (pH 7.5), 2 mM DTE as equilibration buffer and 50 mM potassium phosphate (pH 7.5), 2 mM DTE, 1 M KCl as elution buffer. The hisactophilin-GFRP fusion protein was purified by nickel affinity chromatography with 20 mM Tris (pH 8.0), 500 mM NaCl, 10 mM  $\beta$ -mercaptoethanol (ME) as equilibration buffer and 20 mM Tris (pH 8.0), 500 mM NaCl, 500 mM imidazole, 10 mM  $\beta$ -ME as elution buffer.

The reaction mixture for the determination of GTP cyclohydrolase I activity<sup>19</sup> contained 50 mM Tris-HCl (pH 7.5), 1 mM GTP and recombinant GTP cyclohydrolase I. The reaction mixture for the complex contained 50 mM Tris-HCl (pH 7.5), 1 mM GTP, 400  $\mu$ M BH<sub>4</sub>, recombinant GTP cyclohydrolase I and GFRP. The

samples were incubated at 37 °C and absorbance at 330 nm was recorded. The concentration of 7,8-dihydro-neopterin triphosphate was estimated using the absorption coefficient of  $\epsilon = 6300 \text{ M}^{-1}$ .

#### Total reflection X-ray fluorescence

Total reflection X-ray fluorescence using a Atomica (Oberschleißheim, Germany) spectrometer was applied to investigate the nature of the bound ion. Protein solution (5  $\mu$ l of 5 mg/ml in 100 mM potassium phosphate (pH 7.5)) that was purified as described above were used to measure X-ray fluorescence. No metal ion apart from potassium could be identified in any of the measurements.

#### Crystallisation and data collection

GFRP was crystallised in a batch procedure. The recombinant protein was concentrated in the gel filtration buffer (100 mM potassium phosphate, 2 mM dithiothreitol (pH 7.4)) up to 5 mg/ml. Crystallisation was observed at 4 °C overnight and produced long needles with dimensions 0.1 mm  $\times$  0.1 mm  $\times$  1.0 mm. Crystals belonged to space group  $P2_12_12$  with unit cell constants  $a = 106.8 \text{ \AA}$ ,  $b = 110.1 \text{ \AA}$ ,  $c = 38.7 \text{ \AA}$ ,  $\alpha = \beta = \gamma = 90^\circ$  and one pentamer per asymmetric unit. Data to 2.6  $\text{\AA}$  were collected on a MAR Research imaging plate detector with graphite-monochromatised CuK <sub>$\alpha$</sub>  radiation from a Rigaku rotating anode generator

equipped with a Rigaku mirror system. A second crystal form (space group  $I2_13$ , cell axis 146.6 Å) was obtained from 2 M sodium/potassium phosphate, 0.2 M ammonium sulphate, 0.2 M Hepes and diffracted to 3.0 Å.

### Structure determination and refinement

All data were evaluated with DENZO<sup>20</sup> and CCP4 programs.<sup>21</sup> The  $R_{\text{sym}}$  on intensities is 11.8. Multiple isomorphous replacement was used for phase determination by locating heavy-atom sites through difference Patterson methods. Heavy-atom derivatives were prepared by soaking crystals in the mother liquid at 4 °C with either 2 mM thiomersal for 48 hours, 1 mM  $\text{KAu}(\text{CN})_2$  for 24 hours, or 1 mM  $\text{K}_2\text{Pt}(\text{NO}_2)_2(\text{NH}_3)_2$  for 24 hours and interpreted with the PROTEIN program package.<sup>22</sup> Heavy-atom parameters were refined with SHARP<sup>23</sup> and the resulting electron density was solvent flattened with SOLOMON.<sup>24</sup> Optimisation of local symmetry operators, cyclic averaging and model building was done with MAIN,<sup>25</sup> further refinement was done with CNS.<sup>26</sup> The data of the orthorhombic crystal form were refined to an  $R$ -factor of 16.3% ( $R_{\text{free}} = 21.1\%$ ). The r.m.s. deviations from ideal stereochemistry are 0.007 Å for bond lengths and 1.38° for bond angles.  $R_{\text{free}}^{27}$  was calculated using 5% of the reflections. The stereochemistry of the model was verified using PROCHECK.<sup>28</sup> The dihedral angles of the polypeptide backbone are all located within allowed regions of the Ramachandran diagram.<sup>29</sup> The cubic crystal form was solved by molecular replacement and refined to an  $R$ -factor of 21.7% ( $R_{\text{free}} = 26.5\%$ ) with r.m.s. deviations from ideal stereochemistry of 0.011 Å for bond lengths and 1.63° for bond angles.

Figures were prepared using the programs MOLSCRIPT,<sup>30</sup> Raster3D<sup>31</sup> and ALSRIPT.<sup>32</sup> Electrostatic potentials were calculated with Grasp.<sup>33</sup>

### Protein Data Bank accession code

The coordinates and structure factors have been deposited with the RCSB Protein Data Bank under the accession code 1JG5.

## Acknowledgements

This work was supported by European Community grants ERB CHRX CT93-0243 and ERB FMRX-CT98-0204, the Deutsche Forschungsgemeinschaft and the Fonds der chemischen Industrie.

## References

- Nicol, C. A., Smith, G. K. & Dutch, D. S. (1985). Biosynthesis and metabolism of tetrahydrobiopterin and molybdopterin. *Annu. Rev. Biochem.* **54**, 729-764.
- Marletta, M. A. (1994). Nitric oxide synthase: aspects concerning structure and catalysis. *Cell*, **78**, 927-930.
- Kaufmann, S., Pollock, R. J., Summer, G. K., Das, A. K. & Hahra, A. K. (1990). Dependence of an alkyl glycerol-ether monooxygenase activity upon tetrahydrobiopterins. *Biochim. Biophys. Acta*, **1040**, 19-27.
- Xie, L., Smith, J. A. & Gross, S. S. (1998). GTP Cyclohydrolase I inhibition by the prototypic inhibitor 2,4-diamino-6-hydroxypyrimidine. *J. Biol. Chem.* **273**, 21091-21098.
- Niederwieser, A., Blau, N., Wang, M., Joller, P., Atres, M. & Cardesa-Garcia, J. (1984). GTP cyclohydrolase I deficiency, a new enzyme defect causing hyperphenylalaninemia with neopterin, biopterin, dopamin and serotonin deficiencies and muscular hypotonia. *Eur. J. Pediatr.* **141**, 208-214.
- Viveros, O. H., Lee, C.-L., M???, A.-D. M., Nicon, J. C. & Nichol, C. A. (1981). Biopterin cofactor biosynthesis: independent regulation of GTP cyclohydrolase in adrenal medulla and cortex. *Science*, **213**, 349-350.
- Hatakeyama, K., Harada, T. & Kagamiyama, H. (1992). IMP dehydrogenase inhibitors reduce intracellular tetrahydrobiopterin levels through reduction of intracellular GTP levels. *J. Biol. Chem.* **267**, 20734-20739.
- Harada, T., Kagamiyama, H. & Hatakeyama, K. (1993). Feedback regulatory mechanism for the control of GTP cyclohydrolase I activity. *Science*, **260**, 1507-1510.
- Milstien, S., Jaffe, H., Kowlessur, D. & Bonner, T. (1996). Purification and cloning of the GTP cyclohydrolase I feedback regulatory protein, GFRP. *J. Biol. Chem.* **271**, 19743-19751.
- Kapatos, G., Hirayama, K., Shimoji, M. & Milstien, S. (1999). GTP cyclohydrolase I feedback regulatory protein is expressed in serotonin neurons and regulates tetrahydrobiopterin biosynthesis. *J. Neurochem.* **72**, 669-675.
- Imazumi, K., Sasaki, T., Takahshi, K. & Takai, Y. (1994). Identification of a rabphilin-3A-interacting protein as GTP cyclohydrolase I in P12 cells. *Biochem. Biophys. Res. Commun.* **205**, 64-73.
- Laipze, C., Pluss, C., Werner, E., Huwiler, A. & Pfeilschifter, J. (1998). Protein kinase C phosphorylates and activates GTP cyclohydrolase in rat renal mesangial cells. *Biochem. Biophys. Res. Commun.* **251**, 802-805.
- Yoneyama, T., Brewer, J. M. & Hatakeyama, K. (1997). GTP cyclohydrolase I feedback regulatory protein is a pentamer of identical subunits. Purification, cDNA cloning and bacterial expression. *J. Biol. Chem.* **272**, 9690-9696.
- Nar, H., Huber, R., Meining, W., Schmid, C., Weinkauff, S. & Bacher, A. (1995). Atomic structure of GTP cyclohydrolase I. *Structure*, **3**, 459-466.
- Auerbach, G., Hermann, A., Bracher, A., Bader, G., Gütlich, M., Fischer, M. *et al.* (2000). Zinc plays a key role in human and bacterial GTP Cyclohydrolase I. *Proc. Natl Acad. Sci. USA*, **97**, 13567-13572.
- Yoneyama, T. & Hatakeyama, K. (1998). Decameric GTP cyclohydrolase I forms a complex with two pentameric GTP cyclohydrolase I feedback regulatory proteins in the presence of phenylalanine or a combination of tetrahydrobiopterin and GTP. *J. Biol. Chem.* **273**, 20102-20108.
- Gabb, H. A., Jackson, R. M. & Sternberg, M. J. E. (1997). Modelling protein docking using shape complementarity, electrostatics and biochemical information. *J. Mol. Biol.* **272**, 106-120.
- Holm, L. & Sander, C. (1995). Dali: a network tool for protein structure comparison. *Trends Biochem. Sci.* **20**, 478-480.
- Bracher, A., Eisenreich, W., Schranek, N., Ritz, H., Götze, Hermann, A. *et al.* (1998). Biosynthesis of pteridines. NMR studies on the reaction mechanisms of GTP cyclohydrolase I, pyruvoyltetrahydropterin synthase and sepiapterin reductase. *J. Biol. Chem.* **273**, 28132-28141.

20. Otwinowski, Z. & Minor, W. (1997). Processing of X-ray diffraction data collected in oscillation mode. *Methods Enzymol.* **276**, 307-326.
21. Collaborative Computational Project No. 4 (1994). The CCP4 suite: programs for protein crystallography. *Acta Crystallog. sect. D*, **50**, 760-763.
22. Steigemann, W. (1974). Die Entwicklung und Anwendung von rechenverfahren und Rechenprogrammen zur Strukturanalyse von Proteinen am Beispiel des Trypsin-Tyrpsin-inhibitor-komplexes, des freien Inhibitors und der L-Asparaginase. PhD thesis, Technical University of Munich, Munich.
23. La Fortelle, E. & Bricogne, G. (1997). Maximum-likelihood heavy-atom parameter refinement for multiple isomorphous replacement and multiwavelength anomalous diffraction methods. *Methods Enzymol.* **276**, 472-494.
24. Abrahams, J. & Leslie, A. (1996). Methods used in the structure determination of mitochondrial F<sub>1</sub> ATPase. *Acta Crystallog. sect. D*, **52**, 30-42.
25. Turk, D. (1992). Development and usage of a macromolecular graphics program. PhD thesis, Technical University of Munich, Munich.
26. Brünger, A., Adams, P., Clore, G., DeLano, W., Gros, P., Grosse-Kuntleve, R. *et al.* (1998). Crystallography & NMR System: a new software for macromolecular structure determination. *Acta Crystallog. sect. D*, **54**, 905-921.
27. Brünger, A. (1992). Free R value: a novel statistical quantity for assessing the accuracy of crystal structures. *Nature*, **355**, 472-475.
28. Laskowski, R. A., MacArthur, M. W., Moss, D. S. & Thornton, J. M. (1993). PROCHECK: a program to check the stereochemical quality of protein structures. *J. Appl. Crystallog.* **26**, 283-291.
29. Ramachandran, G. N. & Sasisekharan, V. (1968). Conformation of polypeptides and proteins. *Advan. Protein Chem.* **23**, 283-437.
30. Kraulis, P. J. (1991). MOLSCRIPT: a program to produce both detailed and schematic plots of protein structures. *J. Appl. Crystallog.* **24**, 946-950.
31. Merritt, E. A. & Murphy, M. E. P. (1994). Raster3D version 2.0. A program for photorealistic molecular graphics. *Acta Crystallog. sect. D*, **50**, 869-873.
32. Barton, G. J. (1993). ALSRIPT: a tool to format multiple sequence alignments. *Protein Eng.* **6**, 37-40.
33. Nicholls, A., Bharadwaj, R. & Honig, B. (1993). Grasp - graphical representation and analysis of surface properties. *Biophys. J.* **64**, A166.

*Edited by I. Wilson*

(Received 30 May 2001; received in revised form 9 August 2001; accepted 9 August 2001)